

Identification of Potent Inhibitors for Resistant Form of Chronic Myelogenous Leukaemia (CML)

Hemanth Naick Banavath¹, Om Prakash Sharma², Muthuvel Suresh Kumar² and R.Baskaran^{1*}

¹Department of Biochemistry & Molecular biology, School of Life Sciences, Pondicherry University-India

²Centre for Bioinformatics, School of Life Sciences, Pondicherry University-India

Author's name and email id:

1. Hemanth Naick Banavath¹- bhemanthnaick@gmail.com
2. Om Prakash Sharma² - ombioinfo@gmail.com
3. Muthuvel Suresh Kumar² -suresh.bic@pondiuni.com
4. R. Baskaran^{1*} -baskaran.rajasekaran@gmail.com

Abstract. The BCR-ABL protein is the causative agent in the pathogenesis of chronic myeloid leukemia (CML). Although there are several drugs in the market which inhibit BCR-ABL efficiently there are some cases of resistance¹. Imatinib^{2,3}, nilotinib^{3,4}, bosutinib⁴, dasatinib⁵, bafetinib⁶ are approved tyrosine kinase inhibitors (TKI's) and more recently, ponatinib was approved TKI which is shown to bind and inhibit the imatinib resistant BCR-ABL (T315I mutant). Ponatinib showed greater side effects like cardiovascular, cerebrovascular and peripheral vascular thrombosis, including fatal myocardial infarction and stroke⁷. Therefore, there is a need to identify new TKI's which have greater inhibition capacity than marketed TKI's with lesser side effects. In this current study, we have selected mutant BCR-ABL (T315I mutant) as a target protein which constitutes 20% of all mutations and screened several small molecule libraries to investigate the potential drug like compound against the BCR-ABL. Potential drug candidates were further examined for their druggability, stability and binding efficacy using computational approaches. Our investigation showed a group of select lead compounds exhibits promising binding affinity than the existing drugs such as ponatinib, imatinib, dasatinib, nilotinib, bosutinib, bafetinib that may be considered.

Keywords: BCR-ABL, T315I, Active site, Ponatinib, Glide, Virtual screening.

1 Introduction

Chronic myeloid leukemia (CML) is driven by chromosomal aberration called Philadelphia chromosome (Ph). The reciprocal translocation between the Abelson gene on chromosome 9 and break-point cluster region gene on chromosome 22 leads to the formation of Philadelphia chromosome (9; 22) (q34; q11)⁸.

The product of BCR-ABL oncogene (BCR-ABL protein) which is a constitutively active kinase drives the disease CML. BCR-ABL induced CML by phosphorylation of substrate protein Grb2 and many downstream effector molecules⁹. The first tyrosine kinase inhibitor (TKI) imatinib (Gleevec, ST1571), approved by FDA in 2001, has shown a great inhibitory effect on progression of CML¹⁰. Despite imatinib's clinical success, resistance is still a limitation of this drug¹¹. To overcome with this resistance, two second generation TKI's inhibitors, nilotinib (Tasigna, AMN107)¹² and dasatinib¹³ (Sprycel, BMS-354825)¹⁴ were developed, but other forms of resistance still remain, and neither compound inhibits the mutant BCR-ABL, which constitutes 20% of all BCR-ABL mutations¹⁵⁻¹⁷.

Based on the structure based drug design in 2010 ARIAD Pharmaceuticals identified ponatinib which binds to the ATP binding site of mutant BCR-ABL. It was completely active against the mutated BCR-ABL (T315I)¹⁸. Initially, ponatinib was designed to overcome T315I gatekeeper mutation¹⁹. The characteristic feature of ponatinib is to facilitate the carbon-carbon triple bond (ethynyl linkage) between the methyl phenyl and purine groups^{20,21}. Ponatinib holds the Isoleucine side chain without steric interference and there is no loss of a hydrogen bond when Thr315 is mutated to isoleucine¹⁹. Ponatinib binds to BCR-ABL in an imatinib/ nilotinib-like (DFG-out) mode and makes similar interactions, including hydrogen bonds with the main chain carbonyl of Met318, the side chain of Glu286, and main chain amide of Asp381. In addition, the drug makes friendly vanderWaals contacts with Tyr253 & Phe382 because of squeezed conformation of the P-loop and DFG-out mode of activation loop respectively²¹. Ponatinib is also active against many of the other imatinib resistant mutations, including M244V, G250E, Q252H, Y253F/H, E255K/V, F317L, M351T, and F359V, among others²². The activity of ponatinib towards these mutations invokes a similar rationale

as for nilotinib, whereby the drug makes multiple points of contact so that mutation of a residue has less effect on the overall binding affinity of the drug²¹.

The availability of 3D-structure of the target protein and the structural details of ponatinib and T315I mutant Abl protein complex gives us an opportunity to find good biologically active small molecules which actively bind to target.

The present work probed the identification of most potent drug like compound exhibiting better inhibition than ponatinib with the mutated structure of BCR-ABL (T315I). Identified lead molecule was further validated for the structural stability and their binding affinities using MM-GBSA study. The finding of these studies can provide an important clue for the design and development of effective novel TKI inhibitor.

2 Material and Methods

2.1 Protein selection and preparation

The crystallographic co-ordinates for wild (PDB ID: 3OXZ)²³ and mutant type (PDB ID: 3QRJ)²⁴ of BCR-ABL was retrieved Protein Data Bank to their inhibitory effect and further processed for docking purposes Schrödinger²⁵. Water molecules were removed, bond orders were assigned, and hydrogen atoms were added to crystal structures. Further, protein was preprocessed and then reviewed by following the optimization of the target protein. Finally, a restrained minimization of the target structure was performed using the default constraint of 0.30 Å RMSD and the OPLS-2005 force field²⁶.

2.2 Ligand selection and preparation

To find out the potential inhibitors for BCR-ABL, we investigated and annotated various small molecule databases such as Ligand.info: Small-molecule Meta-Database^{27,28} (<http://ligand.info/>) (29,090) DrugBank^{29,30} (6,825), Similar compounds from PubChem³¹ (566). A total number of 36,481 compounds were retrieved from the corresponding databases in Structure Data Format (SDF). Further these small molecules were prepared using the LigPrep wizard of Schrödinger³². Since, collected small molecules doesn't have correct bond orders and bond angles; they

were subjected to full minimization using OPLS_2005²⁶. Physiological pH for protonation states were maintained and realistic bond lengths and bond angles were corrected. Further, Epik^{33,34} option was selected for the accurate enumeration of ligand protonation states in biological condition. Finally, chiralities were determined from the SDF and output was saved in maestro format.

2.3 Receptor Grid generation

Since, glide requires pre-requesting of grid for docking purposes. Grid box was assigned at the center of the ATP binding site of BCR-ABL (T315I) (Glu286, Met318, Ile360, Ala380, Asp381)³⁵ using the “Receptor Grid Generation” of Schrödinger Glide36 so that the ligand can rotate freely inside the binding pocket. The van der Waals (vdW) radii of receptor atoms were scaled by 1.00 Å and partial atomic cutoff 0.25 was added to the system to soften the potential energy of non-polar parts of the protein.

2.4 Virtual Screening

We performed High Throughput Virtual Screening (HTVS) using virtual screening workflow option from Glide. It is an application in maestro software which is used for docking purposes by using different options like HTVS, SP (standard-precision), and XP (extra-precision). Glide performs a complete systematic search of the conformational, orientation, and positional space of the docked ligands. All prepared ligands were incorporated in the Virtual Screening Workflow Wizard. Ligands were further scrutinized for their drug properties using Lipinski rule of five³⁷. Finally, docking was performed by using Glide HTVS in the flexible mode of protein. After, HTVS docking, we kept 10% of the best compounds and these compounds were further assessed in Standard Precision (SP) docking for reliable docking of the selected ligand with high accuracy. Again, the 10% of the successful compounds were further incorporated for XP mode to eliminate the false positives using advanced scoring which results most potent lead molecule.

2.5 Molecular Dynamics Simulation for protein ligand complexes

Protein-ligand complexes were evaluated for their binding stability using Gromacs4.5.5 with the Gromos93al force field³⁸ with our earlier protocol for Protein-ligand complex³⁹. Since, we need a topology file for ligand, ProDRG server⁴⁰ server was used to generate the ligand topology file. Further, these protein ligand complexes were solvated with TIP3P explicit water molecule in a box. Electrostatic energy was calculated using the particle mesh Ewald method⁴¹, which permits the use of the Ewald summation at a computational cost comparable to that of a simple truncation method of 10 Å or less. Linear Constraint Solver (LINCS)⁴² algorithm for covalent bond constraints was used. Before minimization, the system was neutralized by adding 8 Na⁺ ions and then steepest descent approach (1000ps) was used for each protein ligand complex. After energy minimization, equilibration was performed. The system was coupled to the external bath by Berendsen pressure and temperature coupling. Finally, MD run was set to 10 ns with the same parameters as mentioned above for each protein-ligand complexes and trajectories were saved for further analysis using XMGRACE.

2.6 Rescoring of BCR-ABL and drug candidate complexes using interaction energy and MM-GBSA approach

To compute the average interaction energy and binding free energy of seven best lead molecules in complex, interaction energy and Gibbs free energy was calculated. Interaction energy was calculated from BCR-ABL and drug complexes by calculating the short range Lennard-Jones and short range Coulomb energy using the g_energy analysis tool of gromacs software.

$$E_{\text{int}}=E_{\text{LJ}}+E_{\text{Coul}}$$

Here, E_{int} stands for interaction energy, E_{LJ} stands for short ranges Lennard-Jones and E_{coul} denotes short ranges for coulomb energy. It is a crude qualitative estimate of the stability of protein and drug candidate complexes. While the binding free energy is calculated based on the following equation

$$\Delta G_{\text{bind}} = \Delta E_{\text{MM}} + \Delta G_{\text{Solv}} + G_{\text{SA}}$$

Using Schrödinger, Where ΔE_{MM} is the difference in energy between ligand in complex and unliganded receptor⁴³, using the OPLS-AA force-

field. ΔG_{solv} is the difference in the G_{SA} solvation energy of the complex and the sum of solvation energies for the unliganded protein. ΔG_{SA} is the difference in surface area energy for the complex and the sum of surface area energies for the protein and ligand.

3 Results and Discussions

To identify the potential lead compounds, which may have a stronger binding affinity to the ATP binding site of BCR-ABL, better than existing drug compound we performed High throughput virtual screening of the T315I Mutant (PDB:3QRJ) BCR-ABL against various small molecule libraries. Ponatinib, bosutinib, bafetinib, dasatinib, nilotinib and imatinib were selected as a reference compounds to set the cutoff value for XP docking. Docking experiment was performed with the mutant type of the target protein. Our docking study showed that ponatinib has the highest binding affinity to inhibit the drug target with the docking score of -11.050kcal/mol while bosutinib, bafetinib, dasatinib, nilotinib and imatinib showed -5.513kcal/mol, -4.689kcal/mol, -4.702kcal/mol, -3.772kcal/mol, -3.593kcal/mol and -3.78kcal/mol, respectively (Table 1). Hence, for screening potent lead molecules, we set -11.00 kcal/mol, as a cutoff value.

Our virtual screening experiment yielded seven persuasive lead compounds, four lead molecules (DB07107, DB06977, DB04200 and DB01172) from DrugBank and three lead molecule from ligand info. Database (ST007180, ST013616 and ST019342). All seven lead molecules exhibited enhanced binding affinity than reference drug molecules. Their 2D conformations and drug details are summarized in Table 2.

DB07107 (C23H22N4O) from DrugBank showed highest binding energy with the XP Score of -14.045 kcal/mol which is greater than our selected cutoff value (Figure 1a). To get an insight into their interacting mechanism, we used UCFC Chimera molecular visualization tool^{44,45} and glide for generating 2D interaction plot. Detailed analysis of this docking pose revealed four hydrogen bonds (H_bonds) interactions with the ATP binding site residues of BCR-ABL. Here, we observed single H_bond with each Glu286 and Met318 residues with bond length of 2.92Å and 2.97Å, while two H_bond formation was encountered with Asp381 with the bond length of 3.32Å, 2.72Å respectively.

DB06977 (C23H21N5O), ST013616 (C14H12N4O2) (Figure 1b,1c), DB04200 (C20H22O6), ST007180 (C18H17FN2OS), ST019342

(C₁₅H₁₁ClO₄) and DB01172 (C₁₈H₃₆N₄O₁₁) (Figure 2) showed a strong binding affinity with XP score of -13.163kcal/mol, -12.065kcal/mol, -12.041kcal/mol, -11.555kcal/mol, -11.033 kcal/mol and -8.433kcal/mol respectively (Table 3) with the key residues of Glu286, Meth318 and Asp381. Here, it is noticeable that DB01172 exhibits XP docking score below the cutoff value but showed higher binding affinity towards the BCR-ABL, and hence was included for further study. DB01172 shares six H₂O bonds with the ATP binding site of the target protein. Moreover, DB01172 forms each one side chain hydrogen bond with Glu282, Glu286, Asp381, Lys285, and one back bone hydrogen bonding each with Asp381, Ile360.

3.1 Validation of drug candidate in Wild type

To evaluate the efficiency of the selected compounds with the wild type of BCR-ABL (PDB: 3OXZ), we performed docking study as mentioned in above protocol and the results were summarized in Table 4. Result showed high inhibitory activity with wild type and mutant. DB07107, ST013616, DB04200 and ST007180 displayed docking score better than ponatinib and imatinib. In case of DB06977, one H₂O bond is missing (Met318) in the wild type of Bcr-Abl but still exhibits favourable binding score of -10.94 kcal/mol, while in case of ST013616, there is loss of one H₂O bond with Asp381. In addition, DB06977 makes one extra H₂O bond with Lys271. Most of selected drug in these study have shown slightly less efficiency in wild type compare to mutant T315I mutant Bcr-Abl. These investigations showed that the selected drugs can efficiently inhibit both mutant and wild type Bcr-Abl.

3.2 Molecular Dynamics Simulations

Based on the virtual screening result, MD Simulation was carried out for the best nine molecules complexes with BCR-ABL using Gromacs4.5.5. The structural behaviour of protein-ligand complexes was studied in a dynamic context, especially in terms of complex flexibility. Root mean square deviations of each protein-ligand complexes have not shown much variation in their backbone. Initially, each lead molecule was in excited state and they exhibited RMSD energy of 0.1500 nm to 0.3 nm. DB01172 have shown continuous fluctuation up to 6000 ps, afterwards it maintains its equilibration state. None of the lead molecules have major

RMSD fluctuations during the trajectory period of simulation indicating that ligands are not playing a major role for the structural stability of the protein backbone and the whole system is stable and well equilibrated (Figure 3).

To investigate the total drift in the RMSD of ligands behavior, we generated the ligand positional RMSD of each lead molecule⁴⁶. ST019342 compound showed more and continues fluctuations in the noticeable window size of 0.4 nm throughout the simulation period. ST019342-BCR-ABL complex co-ordinates were downloaded from the system in the interval of 1000 ps and investigated in PyMOL. Result showed that ST019342 has an unstable binding affinity toward BCR-ABL as the drug was coming out from the binding pocket of the target protein and exhibiting more fluctuation. This suggests that ST019342 compound's inability to inhibit the protein target efficiently while the other drug candidates showed stable and well equilibrated binding (Figure 4).

Residual mobility was calculated using the Root Mean Square Fluctuation (RMSF) and graph was plotted against the residue number based on the trajectory period of MDS. The general profile of residual fluctuation was minimal since there was no abnormal fluctuation (Figure 5). In sum, none of the drug candidates brought any noticeable changes in their residual level.

3.3 Hydrogen bond analysis

MD analysis of BCR-ABL and selected drug candidates complex stability was monitored during the trajectory period and their hydrogen bonds between protein and ligands were calculated using the `g_hbond` utility of GROMACS to determine the stability of hydrogen bonds with the ATP binding site of T315I.

Hydrogen bond analysis reveals that compound DB01172 has 6-7 (highest) number of average H_bonds (Glu282, Lys285, Glu286, Ile360) and two H_bond with Asp381 (Figure 6). Whereas Compounds DB07107, DB06977, ST013616, DB04200, ST007180 and ST019342 showed an average number of hydrogen bond 2-3 (Glu286, Met318 and Asp381), 3 (Glu286, Met318 and Asp381), 3-4 (Glu286, Asp381, Glu316, Met318), 2-3 (Glu286 and Met318), 1 (322) and 1-2 (Met318 and Asn322) respectively (Figure 7). These average number of H_bonds throughout the MDS period provides stability to the protein and ligand complex and holding it to the ATP binding position.

3.4 Interaction energy and binding free energy

Interaction energy and MM-GBSA of BCR-ABL with drug complexes were also calculated. The data showed that all the selected drug compounds have superior interaction energy of -64.37kcal/Mol, -44.58kcal/mol and -42.62kcal/mol for DB06977, DB07107 and DB04200, respectively. Interestingly, DB01172 showed the highest crude interaction energy of -65.490 kcal/mol. Re-scoring of the complexes using Prime MM-GBSA results that all the selected drug candidates display excellent binding free energy (Table 5). Since DB07107, DB06977, DB04200, ST17180 and DB01172 showed promising results in all the above mentioned experiments these drugs can effectively inhibit BCR-ABL kinase activity by blocking the DFG out conformation of BCR-ABL (Figure 8). We strongly recommend these compounds to be tested experimentally for further verification. ST019342 and ST013616 showed poor interaction and binding free energy. Moreover, the backbone of these drug compounds are not stable throughout the simulation period and hence unlikely to be a potent inhibitor of BCR-ABL.

4 Conclusions

In this current study we performed the docking study against the T315I mutant tyrosine kinase to inhibit the chronic myelogenous leukemia (CML) using virtual screening approach. The study yielded highly potential seven lead molecules which were further scrutinized for the structural and binding affinities using MDS and interaction energy. MDS study illustrated the dynamic behaviour of protein-ligand complexes. Specifically, DB07107, DB06977, ST013616, DB04200, ST007180 and DB01172 showed minimal protein backbone and ligand backbone fluctuation whereas ST019342 showed an abnormal fluctuation throughout the simulation study and ligand is not stable inside the binding pocket. Hydrogen bond analysis revealed that DB01172 has high binding affinity towards the binding pockets. Moreover, this particular compound exhibits average of six hydrogen bonds with the protein complex throughout the trajectory period while other compound such as DB06977 and ST013616 showed average of three H₂O bond interactions with BCR-ABL protein. Prime MM-GBSA investigations revealed that all the selected

lead molecules possess good free binding energy and interestingly DB01172 shows greater crude interaction energy when compared to all other lead molecules. Hence, we propose DB07107, DB06977, DB04200, ST007180 and DB01172 to be tested experimentally for further analysis as a highly potential drug candidate for blocking BCR-ABL towards the treatment of chronic myeloid leukemia (CML).

5 Acknowledgements

The Authors thanks to the Pondicherry University to the financial assistant to carry out this work. Hemanth Naick Banavath is thankful to University Grants Commission, India for BSR Meritorious research Fellowships to pursue the Ph.D. Support for Om Prakash Sharma was provided by the Council of Scientific & Industrial Research (CSIR), India for the Senior Research Fellowship (09/559/(0085)/2012/EMR-I) to pursue the Ph.D degree. Research work was carried out at the Laboratory of the Centre for Excellence in Bioinformatics and Department of Biochemistry & Molecular Biology, Pondicherry University, India.

6 References

1. H. M. Kantarjian, M. Talpaz, F. Giles, S. O'Brien and J. Cortes, *Annals of internal medicine*, 2006, 145, 913-923.
2. X. An, A. K. Tiwari, Y. Sun, P. R. Ding, C. R. Ashby, Jr. and Z. S. Chen, *Leukemia research*, 2010, 34, 1255-1268.
3. R. Ren, *Nature reviews. Cancer*, 2005, 5, 172-183.
4. P. W. Manley, N. Stiefl, S. W. Cowan-Jacob, S. Kaufman, J. Mestan, M. Wartmann, M. Wiesmann, R. Woodman and N. Gallagher, *Bioorganic & medicinal chemistry*, 2010, 18, 6977-6986.
5. J. Das, P. Chen, D. Norris, R. Padmanabha, J. Lin, R. V. Moquin, Z. Shen, L. S. Cook, A. M. Doweyko, S. Pitt, S. Pang, D. R. Shen, Q. Fang, H. F. de Fex, K. W. McIntyre, D. J. Shuster, K. M. Gillooly, K. Behnia, G. L. Schieven, J. Wityak and J. C. Barrish, *Journal of medicinal chemistry*, 2006, 49, 6819-6832.
6. A. Yokota, S. Kimura, S. Masuda, E. Ashihara, J. Kuroda, K. Sato, Y. Kamitsuji, E. Kawata, Y. Deguchi, Y. Urasaki, Y. Terui, M.

- Ruthardt, T. Ueda, K. Hatake, K. Inui and T. Maekawa, *Blood*, 2007, 109, 306-314.
7. M. Razzak, *Nature reviews. Clinical oncology*, 2013, 10, 65.
 8. A. Quintas-Cardama and J. Cortes, *Blood*, 2009, 113, 1619-1630.
 9. A. M. Pendergast, L. A. Quilliam, L. D. Cripe, C. H. Bassing, Z. Dai, N. Li, A. Batzer, K. M. Rabun, C. J. Der, J. Schlessinger and et al., *Cell*, 1993, 75, 175-185.
 10. R. Capdeville, E. Buchdunger, J. Zimmermann and A. Matter, *Nat Rev Drug Discov*, 2002, 1, 493-502.
 11. T. O'Hare, C. A. Eide and M. W. Deininger, *Blood*, 2007, 110, 2242-2249.
 12. E. Weisberg, P. W. Manley, W. Breitenstein, J. Bruggen, S. W. Cowan-Jacob, A. Ray, B. Huntly, D. Fabbro, G. Fendrich, E. Hall-Meyers, A. L. Kung, J. Mestan, G. Q. Daley, L. Callahan, L. Catley, C. Cavazza, M. Azam, D. Neuberg, R. D. Wright, D. G. Gilliland and J. D. Griffin, *Cancer Cell*, 2005, 7, 129-141.
 13. C. L. Sawyers, *The New England journal of medicine*, 2010, 362, 2314-2315.
 14. N. P. Shah, C. Tran, F. Y. Lee, P. Chen, D. Norris and C. L. Sawyers, *Science*, 2004, 305, 399-401.
 15. T. O'Hare, D. K. Walters, E. P. Stoffregen, T. Jia, P. W. Manley, J. Mestan, S. W. Cowan-Jacob, F. Y. Lee, M. C. Heinrich, M. W. Deininger and B. J. Druker, *Cancer Res*, 2005, 65, 4500-4505.
 16. Y. Deguchi, S. Kimura, E. Ashihara, T. Niwa, K. Hodohara, Y. Fujiyama and T. Maekawa, *Leuk Res*, 2008, 32, 980-983.
 17. S. Redaelli, R. Piazza, R. Rostagno, V. Magistroni, P. Perini, M. Marega, C. Gambacorti-Passerini and F. Boschelli, *J Clin Oncol*, 2009, 27, 469-471.
 18. T. O'Hare, R. Pollock, E. P. Stoffregen, J. A. Keats, O. M. Abdullah, E. M. Moseson, V. M. Rivera, H. Tang, C. A. Metcalf, 3rd, R. S. Bohacek, Y. Wang, R. Sundaramoorthi, W. C. Shakespeare, D. Dalgarno, T. Clackson, T. K. Sawyer, M. W. Deininger and B. J. Druker, *Blood*, 2004, 104, 2532-2539.
 19. T. O'Hare, W. C. Shakespeare, X. Zhu, C. A. Eide, V. M. Rivera, F. Wang, L. T. Adrian, T. Zhou, W. S. Huang, Q. Xu, C. A. Metcalf, 3rd, J. W. Tyner, M. M. Loriaux, A. S. Corbin, S. Wardwell, Y. Ning, J. A. Keats, Y. Wang, R. Sundaramoorthi, M. Thomas, D. Zhou, J. Snodgrass, L. Commodore, T. K. Sawyer, D. C. Dalgarno, M. W.

- Deininger, B. J. Druker and T. Clackson, *Cancer cell*, 2009, 16, 401-412.
20. O. Frankfurt and J. D. Licht, *Clinical cancer research : an official journal of the American Association for Cancer Research*, 2013, 19, 5828-5834.
 21. E. P. Reddy and A. K. Aggarwal, *Genes & cancer*, 2012, 3, 447-454.
 22. T. O'Hare, C. A. Eide, J. W. Tyner, A. S. Corbin, M. J. Wong, S. Buchanan, K. Holme, K. A. Jessen, C. Tang, H. A. Lewis, R. D. Romero, S. K. Burley and M. W. Deininger, *Proc Natl Acad Sci U S A*, 2008, 105, 5507-5512.
 23. T. Zhou, L. Commodore, W. S. Huang, Y. Wang, M. Thomas, J. Keats, Q. Xu, V. M. Rivera, W. C. Shakespeare, T. Clackson, D. C. Dalgarno and X. Zhu, *Chem Biol Drug Des*, 2011, 77, 1-11.
 24. W. W. Chan, S. C. Wise, M. D. Kaufman, Y. M. Ahn, C. L. Ensinger, T. Haack, M. M. Hood, J. Jones, J. W. Lord, W. P. Lu, D. Miller, W. C. Patt, B. D. Smith, P. A. Petillo, T. J. Rutkoski, H. Telikepalli, L. Vogeti, T. Yao, L. Chun, R. Clark, P. Evangelista, L. C. Gavrilescu, K. Lazarides, V. M. Zaleskas, L. J. Stewart, R. A. Van Etten and D. L. Flynn, *Cancer Cell*, 2011, 19, 556-568.
 25. R. A. Friesner, J. L. Banks, R. B. Murphy, T. A. Halgren, J. J. Klicic, D. T. Mainz, M. P. Repasky, E. H. Knoll, M. Shelley, J. K. Perry, D. E. Shaw, P. Francis and P. S. Shenkin, *J Med Chem*, 2004, 47, 1739-1749.
 26. J. L. Banks, H. S. Beard, Y. Cao, A. E. Cho, W. Damm, R. Farid, A. K. Felts, T. A. Halgren, D. T. Mainz, J. R. Maple, R. Murphy, D. M. Philipp, M. P. Repasky, L. Y. Zhang, B. J. Berne, R. A. Friesner, E. Gallicchio and R. M. Levy, *Journal of computational chemistry*, 2005, 26, 1752-1780.
 27. M. von Grotthuss, J. Pas and L. Rychlewski, *Bioinformatics*, 2003, 19, 1041-1042.
 28. M. von Grotthuss, G. Koczyk, J. Pas, L. S. Wyrwicz and L. Rychlewski, *Comb Chem High Throughput Screen*, 2004, 7, 757-761.
 29. C. Knox, V. Law, T. Jewison, P. Liu, S. Ly, A. Frolkis, A. Pon, K. Banco, C. Mak, V. Neveu, Y. Djoumbou, R. Eisner, A. C. Guo and D. S. Wishart, *Nucleic acids research*, 2011, 39, D1035-1041.
 30. D. S. Wishart, C. Knox, A. C. Guo, D. Cheng, S. Shrivastava, D. Tzur, B. Gautam and M. Hassanali, *Nucleic acids research*, 2008, 36, D901-906.

31. Y. W. Evan E. Bolton¹, Paul A. Thiessen¹, Stephen H. Bryant¹ *
Annual Reports in Computational Chemistry, 4.
32. v. Schrödinger Release 2013-2: LigPrep, Schrödinger, LLC, New York, NY, 2013.
33. J. R. Greenwood, D. Calkins, A. P. Sullivan and J. C. Shelley, Journal of computer-aided molecular design, 2010, 24, 591-604.
34. Epik, version 2.3, Schrödinger, LLC, New York, NY, 2012.
35. M. J. Eck and P. W. Manley, Current opinion in cell biology, 2009, 21, 288-295.
36. R. A. Friesner, R. B. Murphy, M. P. Repasky, L. L. Frye, J. R. Greenwood, T. A. Halgren, P. C. Sanschagrin and D. T. Mainz, J Med Chem, 2006, 49, 6177-6196.
37. C. A. Lipinski, F. Lombardo, B. W. Dominy and P. J. Feeney, Advanced drug delivery reviews, 2001, 46, 3-26.
38. D. Van Der Spoel, E. Lindahl, B. Hess, G. Groenhof, A. E. Mark and H. J. Berendsen, Journal of computational chemistry, 2005, 26, 1701-1718.
39. O. P. Sharma, Y. Vadlamudi, Q. H. Liao, B. Strodel and M. S. Kumar, J Biomol Struct Dyn, 2013, 31, 765-778.
40. A. W. Schuttelkopf and D. M. van Aalten, Acta crystallographica. Section D, Biological crystallography, 2004, 60, 1355-1363.
41. H. Wang, F. Dommert and C. Holm, The Journal of chemical physics, 2010, 133, 034117.
42. S. Amiri, M. S. Sansom and P. C. Biggin, Protein engineering, design & selection : PEDS, 2007, 20, 353-359.
43. Prime, version 3.0, Schrödinger, LLC, New York, NY, 2011, 2011.
44. C. C. Huang, Couch, G.S., Pettersen, E.F., and Ferrin, T.E., Pacific Symposium on Biocomputing, 1996, 1, 724.
45. M. F. Sanner, A. J. Olson and J. C. Spehner, Biopolymers, 1996, 38, 305-320.
46. O. P. Sharma, A. Pan, S. L. Hoti, A. Jadhav, M. Kannan and P. P. Mathur, Med Chem Res, 2012, 21, 2415-2427.

7 Tables

Table 1. Glide XP results for the existing drug molecules for mutant BCR-ABL, by Schrödinger 9.3.

Pubchem ID	Name	Docking Score	Glide Score	HD:HA(Å)
24826799	Ponatinib	-11.917	-11.050	Glu286:oe2::n3(2.865) Met318:n::n5(2.815) Ile360:o::n2(3.457) Asp381:n::o1(2.867)
5328940	Bosutinib	-5.310	-5.513	Asp381:od2::n2(2.737) Ile360:n::n5(3.047)
24853523	Bafetinib	-4.644	-4.644	Asp381:o::n3(2.720) Arg362:nh2::n8(3.223)
3062316	Dasatinib	-4.220	-4.702	Ile360:o:o1(2.827) Arg362:nh1::o1(2.959) Ile360:n::o1(3.095)
644241	Nilotinib	-3.617	-3.772	Arg362:nh1::o1(2.810) Asp381:od2:n2(3.029)
5291	Imatinib	-3.460	-3.593	Glu292:oe2::n2(3.092) Ile360:o::n4(3.027)

Table 2. 2-D Structures of the finally selected seven lead molecules have been shown in the figure. (a) DB07107 (b) DB06977, (c) ST013616, (d) DB04200, (e) ST007180, (f) ST019342 and (g) DB01172.

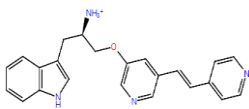
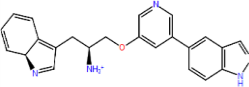
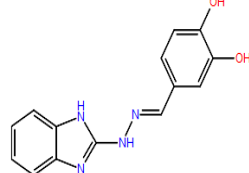
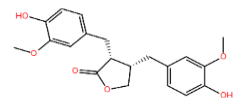
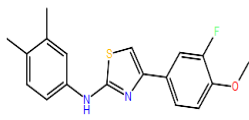
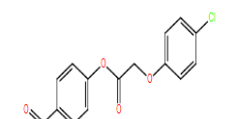
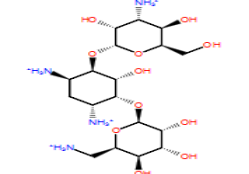
DrugBank ID (PubChem ID)	Chemical Formula	Molecular weight	2D-Structure
DB07107 (6914613)	C ₂₃ H ₂₂ N ₄ O	370.447	
DB06977 (46937040)	C ₂₃ H ₂₁ N ₅ O	383.446	
ST013616 (6530845)	C ₁₄ H ₁₂ N ₂ O ₂	268.270	
DB04200 (119205)	C ₂₀ H ₂₂ O ₆	358.385	
ST007180 (2057417)	C ₁₈ H ₁₇ N ₂ O ₂ S	328.403	
ST019342 (670959)	C ₁₅ H ₁₁ ClO ₄	290.698	
DB01172 (6032)	C ₁₈ H ₃₆ N ₄ O ₁₁	484.498	

Table 3. Glide XP results for the seven lead molecules with the Mutant type of BCR-ABL , by Schrödinger 9.3

Drug Bank ID	Docking Score	Glide Score	HD:HA(Å)
DB07107	-14.031	-14.045	Glu286:OE2:: N4(2.92), Met318:N:: N1 (2.97), Asp381:O1:: N(3.32), Asp381:N4:: O (2.72)
DB06977	-13.163	-13.163	Glu286:Oe2 :: N5(2.81), Glu381:N5:: O (2.73), Met318:O:: N3(3.08)
ST013616	-12.106	-12.041	Glu286:OE2:: O1(2.79), Met381:O2:: O(2.96), Glu316:O: N2 (3.41), Met318:N:: N3(3.07)
DB04200	-12.065	-12.065	Glu286:OE2::O5(2.78), Met318: N:: O2 (3.07), Met318:N::O1(3.33)
ST007180	-11.555	-11.555	Asn322 ND2: O1 (2.79)
ST019342	-11.033	-11.033	Met318 N1: N (2.84), Asn322 N: O4 (3.41) Asn322 Nd2 : O4 (2.75)
DB01172	-8.603	-8.433	Glu282 OE1: N4 (2.66), Lys285 O: N3 (3.52), Glu286 OE2: N2 (3.03), Ile360 O: N1 (2.82), Asp381 OD2: O4 (2.84), Asp381 O: N2 (3.10)

Table 4. Glide XP results for the seven lead molecules with the wild type of BCR-ABL, by Schrödinger 9.3.

Compound	XP Score (Wild)	Amino acid interactions
DB07107	-10.22	Glu286:Oe2::N2(2.658), Asp381:O::N2(2.600), Asp381:N::O1(3.497), Met318:N::N5(3.043)
DB06977	-10.94	Asp381:O::N2(2.599), Glu286:Oe2::N2(2.727)
ST013616	-8.17	Lys 271:N2::O1(3.031), Glu286:Oe2::O2(2.784), Glu286:Oe2::O1(2.627), Glu316:O::N2(3.228), Met318:N::N3(3.020)
DB04200	-9.76	Met318:N::O1(3.177), Asn322:O3::Nd2(2.972) Asp381:O::O6(2.915),
ST007180	-9.62	Met 318:O::N1(3.215), Met 318:O::S1(3.907)
ST019342	-8.33	Met318:N ::O2(3.016), Asn322:Nd2::O4(3.129)
DB01172	-9.72	Ile360:O::O8(2.900), Glu286:Oe2::N2(3.136), Asp381:N::O10(2.787), Asp381:O::O10(3.227), Asp381:Od2::O7(3.486), Glu286:Oe2::O3(2.963), His361:O::N4(2.800), Asp381:Od2::Od2(2.647), Arg362:Nh1::O8(3.365)

Table 5. Interaction energy of each BCR-ABL -ligand complex

Ligand	Average	Err Est	RMSD	Total Drift	Interaction energy	MM- GBSA
DB07107	159619 LJ (SR)	15	1080.95	-94.4324	-44.58	-112.76
	-1.01083e+06 Q(SR)	15	1690.11	-92.1206		
DB06977	159597 LJ (SR)	22	1076.63	-72.1488	-64.37	-126.71
	-1.01083e+06 Q(SR)	44	1679.72	-197.183		
ST013616	237095 LJ(SR)	7.6	1295.91	-28.5264	-25.67	-71.53
	-1.4591e+06 Q(SR)	25	2022.29	-79.4374		
DB04200	159667 LJ (SR)	8.4	1074.5	49.9894	-42.62	-103.15
	-1.4591e+06 Q(SR)	20	1678.84	-128.368		
ST007180	243003 LJ(SR)	20	978.101	-142.857	-58.154	-93.59
	-1.48133e+06 Q(SR)	20	1424.7	-100.463		
ST019342	237089 LJ (SR)	4.3	1300.79	-26.6877	-26.87	-73.73
	-1.45905e+06 Q(SR)	22	2044.03	-85.7545		
DB01172	237089 LJ(SR)	27	1298.3	-156.608	-65.490	- 83.82
	-1.45938e+06 Q(SR)	18	2032.86	-117.406		

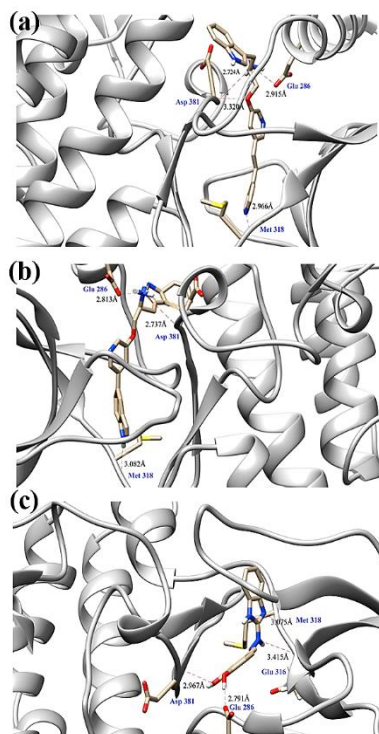


Fig. 1. Binding poses of the DB07107, DB06977, ST013616 lead molecules. The proposed binding mode of the lead molecules has been shown in the stick format. Residues involved in Hydrogen bonding have been labeled with the Hydrogen bond in dotted red lines and bond length have been shown in Angstrom.

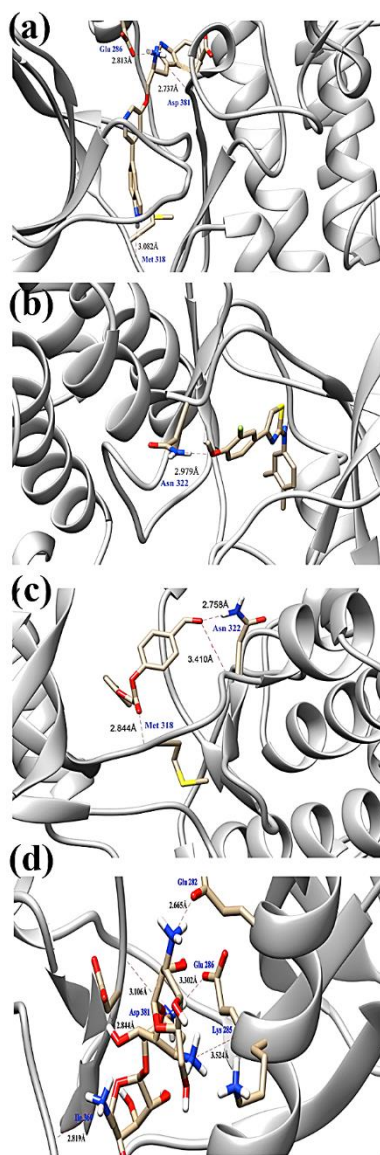


Fig. 2. Binding poses of the DB04200, ST007180, ST019342 and DB01172 lead molecules. The proposed binding mode of the lead molecules has been shown in the stick format. Residues involved in Hydrogen bonding have been labeled with the Hydrogen bond in dotted red lines and bond length have been shown in Angstrom.

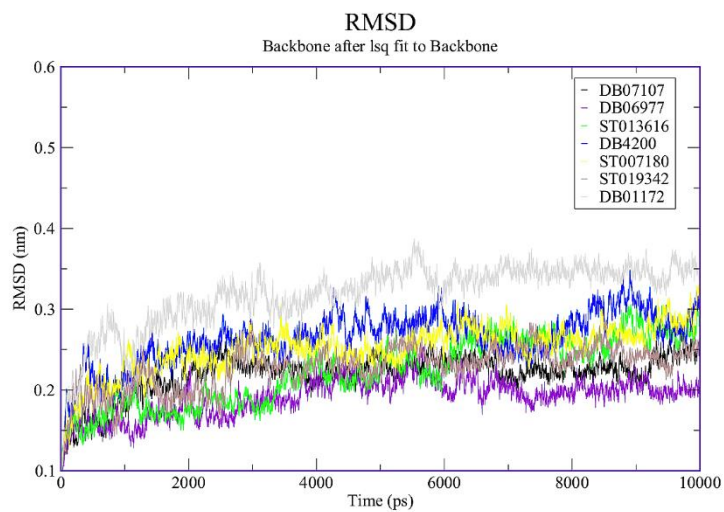


Fig. 3. Time dependence of root mean square deviations (RMSDs). Backbone RMSD from the initial structures of protein-ligand complexes during 10,000 ps molecular dynamics (MD) simulation.

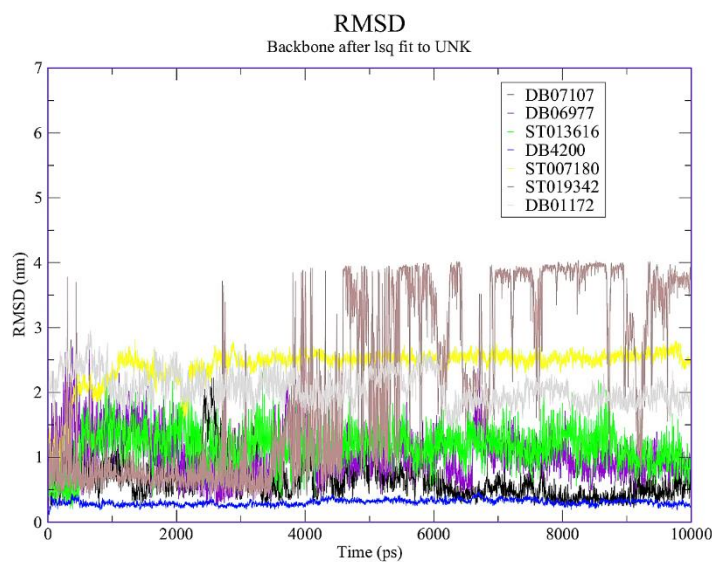


Fig. 4. Backbone RMSD values of drug candidates from the initial structures of protein-ligand complexes during 10,000 ps of molecular dynamics (MD) simulation period. Graphs were plotted using xmgrace, a 3D plotting tool.

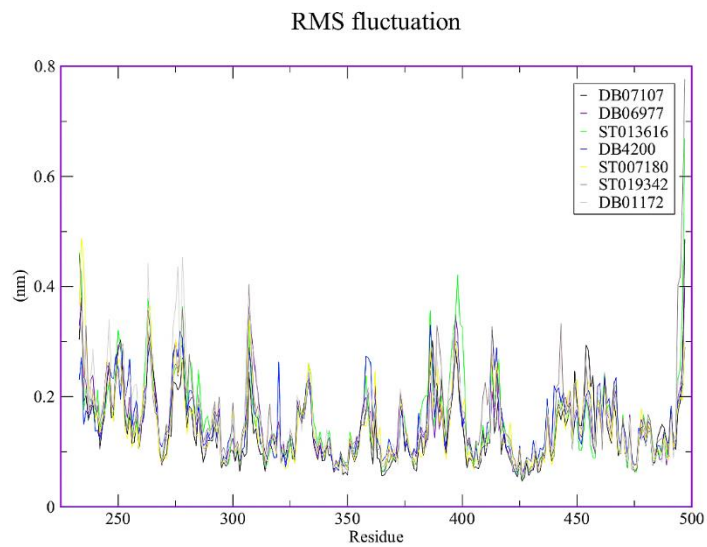


Fig. 5. Root mean square fluctuations (RMSF) from the initial structures of protein-ligand complexes during the trajectory period of simulation.

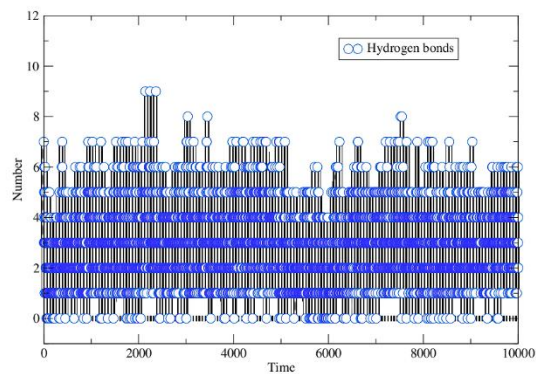


Fig. 6. Total number of inter-molecular H_bond interactions between BCR-ABL and DB01172 lead molecules.

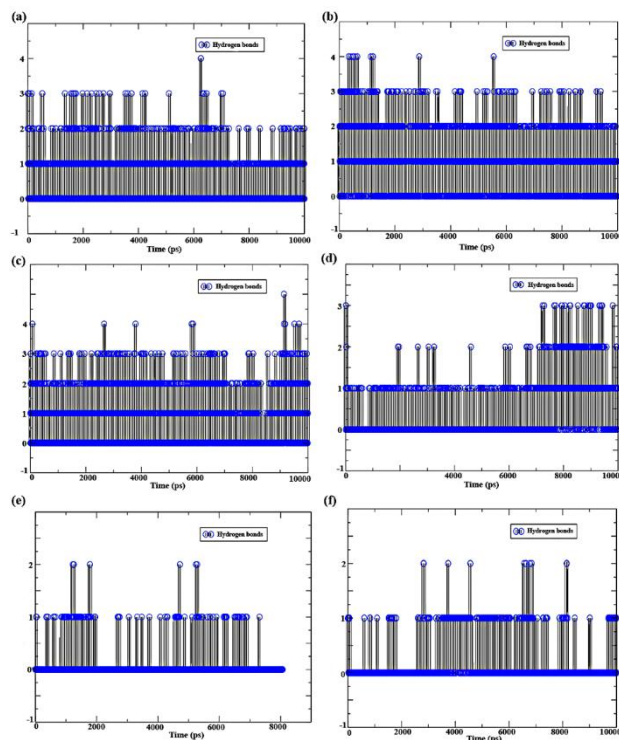


Fig. 7. Total number of inter-molecular H₂O interactions between BCR-ABL and DB07107, DB06977, ST013616, DB04200, ST007180 and ST019342 lead molecules.

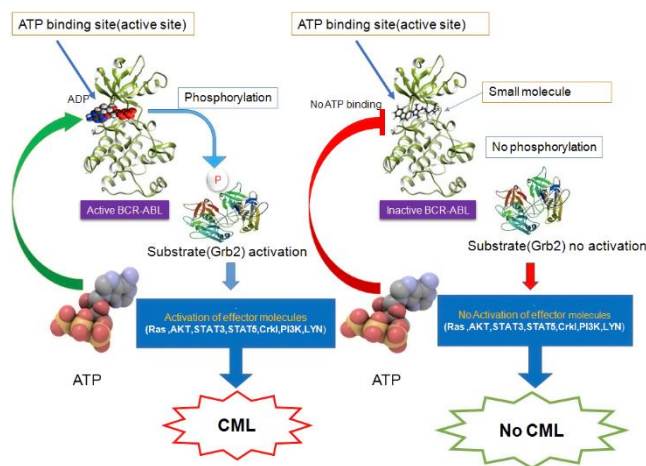


Fig. 8. Mechanism of BCR-ABL inhibition by selected lead compounds.